Bonding of H_2, N_2, Ethylene, and Acetylene to Bivalent Lanthanide Metallocenes: Trends from DFT Calculations on Cp_2M and Cp^*_2M (M = Sm, Eu, Yb) and Experiments with Cp^*_2Yb

L. Perrin,[†] L. Maron,*[,‡] O. Eisenstein,*[,†] D. J. Schwartz,[§] C. J. Burns,[§] and R. A. Andersen*[,§]

LSDSMS (UMR 5636), Université Montpellier 2, 34095 Montpellier Cedex 05, France, Laboratoire de Physique Quantique (UMR 5626), IRSAMC, Université Paul Sabatier, 118 route de Narbonne, 31064 Toulouse Cedex 04, France, and Chemistry Department and Chemical Sciences Division of Lawrence Berkeley National Laboratory, University of California, Berkeley, California 94720

Received September 29, 2003

The results of DFT calculations have been used to define the trends in the interactions of H_2, N_2, C_2H_4, C_2H_2, and C_2Me_2 with the bivalent lanthanide metallocenes Cp_2M (Cp = η^5-C_5H_5) and Cp^*_2M ($Cp^* = \eta^5$-C_5Me_5), where M = Sm, Eu, Yb. These results, together with those previously published for the bonding of CO to Cp_2M (M = Ca, Eu, Yb), suggest that the interaction of these ligands with the lanthanide metallocenes results from a subtle balance between attractive (dipole−dipole or dipole−induced dipole) and repulsive (electron−electron repulsion within the f shell) forces. The balance between the attractive and repulsive forces, and therefore the net bond energy, depends on the f-electron count in these bivalent lanthanide metallocenes. The computational results are compared with experimental observations on paramagnetic Cp^*_2Eu and diamagnetic ytterbocene, Cp^*_2Yb.

Introduction

It has been shown recently that the CO pressure and temperature dependence for the equilibrium reaction between CO and Cp^*_2M ($Cp^* = \eta^5$-C_5Me_5; M = Ca, Eu) in hydrocarbon solution yields a monocarbonyl adduct with a change in enthalpy of about −4 kcal mol^{-1}.[1] For Ca and Eu, the CO stretching frequency of the 1:1 adduct is greater than that of free CO. In contrast, for Yb, an equilibrium exists between 1:1 and 1:2 adducts, both of which have CO stretching frequencies lower that that of free CO.[1] DFT calculations model properly the experimental variation ($\Delta\nu_{CO}$) of CO stretching frequencies relative to that of free CO for $Cp_2M(CO)$ (Cp = η^5-C_5H_5), when M is Ca or Eu and when the CO ligand is C-bound. In the case of Cp_2Yb, the experimental lowering of the CO stretching frequencies is properly reproduced only for an O-bonded carbon monoxide in both adducts.[2] The principle that emerges from the DFT calculations is that π-back-bonding from the 4f core electrons is not involved in the bond to CO. The bonding between Cp_2M and CO is the result of dipole−dipole interactions along with a small amount of charge transfer from CO to Cp_2M; the charge transfer is responsible for electron−electron (e−e) repulsion with the electrons in the f shell. In the case of Cp_2Eu ($4f^7$) the increase in the e−e repulsion with the half-filled 4f shell is less than the attractive forces, resulting in a net bond between Cp_2Eu and CO. In the case of Cp_2Yb ($4f^{14}$) the increase in e−e is larger with the full 4f shell, which is minimized when the electronegative end (viz., the oxygen atom) of CO binds to the metal center. This results in a lower ν_{CO} value relative to ν_{CO} for free CO, consistent with the experimental result. Thus, the Cp_2M fragment handles the bonding to dipolar CO in different ways, depending upon whether the 4f shell is filled or half-filled. This begets the question of how this bond model can accommodate bonding when the diatomic ligand does not have a permanent dipole moment, the subject of this paper. It is well-known that DFT calculations underestimate dispersion forces.[3] However, this method has been used successfully for metal complexes of rare gas.[4]

Results and Discussion

(I) Molecular Hydrogen and Nitrogen. (a) Experimental Observations. Dihydrogen has been suggested to interact reversibly with Cp^*_2Eu, since the ^1H NMR spectrum shows that the chemical shift of dihy-

[†] Université Montpellier 2.
[‡] Université Paul Sabatier.
[§] University of California.
* Corresponding author.

(1) (a) Schultz, M.; Burns, C. J.; Schwartz, D. J.; Andersen, R. A. *Organometallics* **2001**, *20*, 5690. (b) Selg, P.; Brintzinger, H. H.; Schultz, M.; Andersen, R. A. *Organometallics* **2002**, *21*, 3100.

(2) Perrin. L.; Maron, L.; Eisenstein, O.; Andersen, R. A. *J. Am. Chem. Soc.* **2002**, *124*, 5614.

(3) Wesolowski, T. A.; Parisel, O.; Ellinger, Y.; Weber, J. *J. Chem. Phys. A* **1997**, *101*, 7818.

(4) Andrews, L.; Liang, B. Y.; Li, J.; Bursten, B. E. *J. Am. Chem. Soc.* **2003**, *125*, 3126.

10.1021/om034206v CCC: $25.00
Publication on Web 11/20/2003

Table 1. Calculated Energy Variations and Infrared Stretching Frequency Changes for the Equilibrium $Cp_2M(gas) + L(gas) = Cp_2M{\cdot}L(gas)$[a]

		ΔE (kcal mol^{-1})		$\Delta\nu$ (cm^{-1})	
M	L	Cp	Cp*	Cp	Cp*
Sm	H_2	−0.7		−89	
Eu	H_2	−0.8	0.0	−86	−61
Yb[b]	H_2	−0.5	0.0	−113	−4
Sm	N_2	−4.1		1	
Eu	N_2	−4.2	−3.1	1	−4
Yb	N_2	−4.1	−2.9	−5	−15
Sm	C_2H_4	−6.2		−27	
Eu	C_2H_4	−6.2	−3.9	−26	−21
Yb	C_2H_4	−5.7	−2.9	−29	−24
Sm	C_2H_2	−8.1		−29	
Eu	C_2H_2	−8.2		−29	
Yb	C_2H_2	−7.8		−32	
Eu	C_2Me_2	−7.4	−4.8	−31	−30
Yb	C_2Me_2	−7.0	−3.7	−30	−32

[a] Stretching frequencies for the free ligands (cm^{-1}): H_2, ν_{HH} 4455.6; N_2, ν_{NN} 2.472.7; C_2H_4, ν_{CC} 1717.2; C_2H_2, ν_{CC} 2087.0; C_2Me_2, ν_{CC} 2384.1. [b] See ref 8.

drogen is deshielded in the presence of Cp^*_2Eu.[5] The change in chemical shift of H_2 in the presence of the paramagnetic Cp^*_2Eu relative to that of free H_2 implies that the electron density in the dihydrogen molecule is perturbed on bonding. In contrast, exposure of a solution of Cp^*_2Yb in C_6D_{12} to an atmosphere of either N_2 or H_2 does not perturb the ring resonance of diamagnetic Cp^*_2Yb or that of dissolved H_2 relative to free H_2. In addition, the T_1 value of H_2 is not changed in the presence of Cp^*_2Yb (see the Experimental Section for details). This result might be interpreted to mean that the dihydrogen molecule is perturbed by Cp^*_2Eu but not by Cp^*_2Yb. However, the chemical shift of H_2 induced by the paramagnetic Cp_2*Eu will be larger than that by the diamagnetic Cp^*_2Yb, and no conclusion can be drawn about the relative strength of the interaction.[6]

(b) Computational Studies. The qualitative experimental observations are numerically verified by DFT calculations. As shown in Table 1, the equilibrium reaction of Cp_2M ($Cp = \eta^5$-C_5H_5) with H_2 in the gas phase lies in favor of the H_2 complex by about −0.5 kcal mol^{-1}, for each of the three metallocenes. The calculated changes in the H−H stretching frequency mirror the energy changes.[7] The most important deduction is that Cp_2Eu binds slightly less strongly to H_2 than does Cp_2Yb. The calculations were repeated for the Cp^*_2M fragment in order to examine the change induced by this substitution; these values are listed in Table 1. The donor−acceptor interaction is weaker by about 0.5 kcal mol^{-1} relative to the Cp_2M case, so that ΔE is approximately zero for each of these decamethylmetallocenes.[8]

The calculations were then performed on the equilibrium reaction between Cp_2M and dinitrogen. As shown in Table 1, the energy change for all three metallocenes is favorable by about −4 kcal mol^{-1} in each case, but the perturbation in N−N stretching frequency is small. From consideration of the calculated stretching frequencies, we conclude that the electron density on N_2 is not changed in the presence of the Cp_2M or Cp^*_2M fragments so that a weak adduct, if it exists, should not be spectroscopically detectable. This is consistent with the experimental evidence mentioned above for Cp^*_2Eu and Cp^*_2Yb but contrasts with the published result for Cp^*_2Sm, since the latter gives a 2:1 adduct in which the dinitrogen molecule forms a symmetrical bridge between the two Cp^*_2Sm fragments.[9a] This apparent contradiction between the calculation and experiment can be resolved by postulating that the N_2 compound of Cp^*_2Sm is not an adduct between $Cp^*_2Sm^{II}$ and N_2 but is the result of electron transfer in which two [$Cp^*_2Sm^{III}$] fragments interact with a disordered $[N_2]^{2-}$ fragment. This interpretation is consistent with the recent observation on the 1:2 N_2 adducts of LnX_2 (Ln = Tm, Dy, Nd, X = $NSiMe_3$, $OC_6H_3{}^tBu_2$-2,6).[9b]

(II) Alkene and Alkyne. (a) Experimental Observations. The experimental observation of adduct formation or the lack thereof between Cp^*_2M and nonpolar diatomic molecules (H_2 and N_2) can be extended to simple nonpolar organic molecules such as an alkene or alkyne. An equilibrium reaction between ethylene and Cp^*_2Eu was implied by the change in the ^{1}H NMR chemical shift of the C_2H_4 resonance in the presence of Cp^*_2Eu in C_6D_{12}.[5] In contrast, exposure of Cp^*_2Sm[10a] or Cp^*_2Yb to C_2H_4 in aliphatic hydrocarbon solvent yields polyethylene; see the Experimental Section for details for Cp^*_2Yb. Although mechanistic details are incomplete, adduct formation presumably precedes the electron-transfer event that initiates the polymerization reaction, which has been suggested for bivalent samarium.[10b−e] The adduct between Cp^*_2Yb and MeC≡CMe has been isolated and characterized by X-ray crystallography.[11] In C_6D_6 solution, an equilibrium exists between the adduct and free MeC≡CMe, since the change of the chemical shift in the NMR spectra (^{1}H, ^{13}C) show that electron density in MeC≡CMe is perturbed by Cp^*_2Yb addition. The Experimental Section gives ^{1}H and ^{13}C{^{1}H} NMR chemical shifts of isolated adducts between Cp^*_2Yb and the alkynes PhC≡CPh, MeC≡CPh, and MeC≡CCMe$_3$ in C_6D_6. In each case, the average chemical shifts of the alkyne resonances are perturbed by coordination, but the slow exchange spectra are not obtained by cooling. No experimental studies have been reported for Sm and Eu, but it seems reasonable to assume these two metallocenes would form similar 1:1 adducts.

(5) Nolan S. P.; Marks, T. J. *J. Am. Chem. Soc.* **1989**, *111*, 8538. Eu(II) is 4f^7, and therefore the resonance due to the Cp* hydrogens is not observed in the NMR experiment.

(6) Bertini, I.; Luchinat, C.; Parigi, G. *Solution NMR of Paramagnetic Molecules*; Current Methods in Inorganic Chemistry 2; Elsevier: Amsterdam, 2001.

(7) The calculated changes in stretching frequency upon coordination to the metallocene fragment are more accurate and therefore more trustworthy for the small changes in the values relative to the uncoordinated values. For instance, see ref 4.

(8) In the case of Yb, two minima were located on the potential energy surface, which is correlated with the different conformations (eclipsed and staggered) of the C_5R_5 (R = H, Me) ligand. The energy difference between these two rotamers is small, and the results for the rotamer that is lower in energy (staggered) is listed in Table 1.

(9) (a) Evans, W. J.; Ulibarri, T. A.; Ziller, J. W. *J. Am. Chem. Soc.* **1988**, *110*, 6877. (b) Evans, W. J.; Zucchi, G.; Ziller, J. W. *J. Am. Chem. Soc.* **2003**, *125*, 10.

(10) (a) Evans, W. J.; Decoster, D. M.; Greaves, J. *Macromolecules* **1995**, *28*, 7929. (b) Boffa, L. S.; Novak, B. M. *Tetrahedron* **1997**, *53*, 15367. (c) Ihara, E.; Nodono, M.; Katsura, K.; Adachi, Y.; Yasuda, H.; Yamagashira, M.; Hashimoto, H.; Kanehisa, N.; Kai, Y *Organometallics* **1998**, *17*, 3945. (d) Ihara, E.; Nodono, M.; Katsura, K.; Yasuda, H.; Kanehisa, N.; Kai, Y. *Macromol. Chem. Phys.* **1996**, 197, 1909. (e) Hou, Z.; Zhang, Y.; Tezuka, H.; Xie, P.; Tardif, O.; Koizumi, T.; Yamazabi, H.; Wakatsuki, Y. *J. Am. Chem. Soc.* **2000**, *122*, 10533.

(11) Burns, C. J.; Andersen, R. A. *J. Am. Chem. Soc.* **1987**, *109*, 941.

(b) Computational Studies. Equilibrium adduct formation between Cp_2M and C_2H_4 in the gas phase was explored by calculations, the results of which are shown in Table 1. All three bivalent Cp_2M fragments form adducts with an energy change of about -6 kcal mol^{-1} and a lowering of the C═C stretching frequency by about 30 cm^{-1} for each metallocene. The ethylene adducts are thus energetically favorable, and the changes in $\nu_{C=C}$ parallel the energy change. These trends are maintained for the decamethylmetallocenes. The irreversible polymerization that results in the case of Cp^*_2Sm and Cp^*_2Yb presumably is due to electron transfer after adduct formation. The feasibility of this pathway is related to the reduction potential of the metal fragments (Sm(II) > Yb(II) > Eu(II))[12] and the electron affinity of ethylene; the energy changes in these redox processes are being studied computationally and will be reported at a later date.

The calculated energy change upon reversible binding of Cp_2M or Cp^*_2M and C_2H_2 or C_2Me_2 also is shown in Table 1. In each case, the binding is about 2 kcal mol^{-1} more favorable than for ethylene and the changes in ν_{CC} upon coordination are similar for the ethylene and acetylene adducts. The binding energy for C_2H_2 suggests that an acetylene complex might be isolable, since the calculated free energy changes at 25 °C are -0.8 kcal mol^{-1} for Eu, -0.2 kcal mol^{-1} for Sm, and $+2$ kcal mol^{-1} for Yb: this is indeed the case for Cp^*_2Yb with C_2Me_2.[8]

(III) Bonding Trends. The experimental deductions on the relative binding abilities of the Cp^*_2M fragments toward H_2, N_2, C_2H_4, C_2H_2, and CO[2] are reproduced by calculations on Cp_2M and Cp^*_2M. These calculations support the notion that adduct formation precedes further reactions in the case of Cp^*_2Sm with C_2H_4 and N_2 and of Cp^*_2Yb with C_2H_4. Several patterns emerge from inspection of the values in Table 1. (i) All of the values for the change in energy on adduct formation are small. (ii) The values of ΔE parallel the change in X−X stretching frequency upon binding; a larger change in ΔE correlates with a larger change in $\Delta\nu$. In the cases of binding N_2, C_2H_4, and C_2H_2 (C_2Me_2), ΔE and $\Delta\nu$ follow the order $N_2 < C_2H_4 < C_2H_2$ (C_2Me_2), for a given metallocene. Furthermore, there is no large difference between Sm, Eu, or Yb; however, the trend is for Yb to bond more weakly than the two other metals. Dihydrogen behaves differently with respect to the same set of Cp_2M fragments,[8] since Sm and Eu bind slightly more strongly than Yb and the H_2 stretching frequency is changed more than the stretching frequency of N_2, C_2H_4, and C_2H_2 upon interaction with these metallocenes and decamethylmetallocenes. The correspondence between calculated binding energies and stretching frequencies and the currently available qualitative experimental results shows that the calculations account for the small changes involved when a ligand bonds to these metallocene fragments. The next step in the theoretical treatment is to compare the calculated molecular structures with the experimental results, where the latter are available.

(IV) Adduct Geometry and Bonding. Before discussing the adduct formation between Cp_2M and Cp^*_2M, the geometrical differences between the base-free Cp_2M and Cp^*_2M fragments are described. The Cp(centroid)−metal−Cp(centroid) angle for Cp^*_2M is always larger by 1−2° than for Cp_2M. The metal−Cp(centroid) distance is always shorter for Cp^*_2M by 0.02 Å; the staggered conformation in all cases is the lower minimum.

(a) Dihydrogen. The calculated molecular structures that result from the interaction between Cp_2M and dihydrogen are shown in Figure 1. As dihydrogen approaches the Cp_2M^{II} fragment, the metallocene fragment bends, allowing bonding to develop. The Eu···H distances are longer than the Yb···H distances, and this clearly parallels the change in H_2 stretching frequencies but not the energy,[7] as shown in Table 1. The geometry of adducts in the Cp^*_2M fragment is different from that found in the Cp_2M fragment.[8] The ring(centroid)−M−ring(centroid) angles in the adducts of Cp^*_2M increase by 1−2° relative to those with Cp_2M, and the ring(centroid)−metal distance decreases by 0.02 Å from Cp^*_2M to Cp_2M. The M···H_2 distance increases in the Cp^*_2M adduct relative to the unsubstituted species, and this lengthening parallels the change in ν_{H_2} and binding energy. The M···H_2 distance depends on the metal, as the changes are larger for Yb than for Eu.

The H_2 complex can be used to identify the interactions at work between the ligands and metal fragments studied here. In the d transition metal dihydrogen complexes, the stretching frequency of H_2 is determined by delocalization of the electrons in σ_{H_2} toward the empty metal d orbital and by the back-bonding of the electrons in an occupied metal d orbital toward $\sigma^*_{H_2}$. In the present adducts, the back-bonding is not present.[2] In addition, delocalization of the electron density from the ligand toward the metal is drastically decreased, which appears only in the form of dynamic polarization.[13] Dynamic polarization corresponds to the deformation of the electron cloud in the dihydrogen bond by the electric field created by the dipole moment of Cp_2M and the dihydrogen molecule. Dynamic polarization is expressed as an excitation of the occupied σ_{H_2} toward the empty metal orbitals. This differs from classical ligand to metal charge transfer, which is larger in magnitude than the latter because polarization is exclusively associated with an instantaneous interaction, whereas the traditional charge transfer is associated with an explicit electron transfer. Since only the metal fragment has a permanent dipole, only polarization of the ligand plays a role. Thus, the amount of dynamic polarization increases on raising the energy of the occupied orbitals of the ligand and on increasing the overlap between the orbitals of the two fragments. Static polarization is associated with the occurrence of an induced dipole on the ligand by the electric field of the metallocene. It is expressed in terms of excitation from the occupied orbitals toward the empty orbitals of the ligand itself. This interaction relocalizes the charges within the ligand and thus influences the stretching frequency. It increases with decreasing distances between partners. These properties expressed for H_2 complexes can be generalized to the other ligand systems. Dihydrogen is η^2 bonded with a slight distortion toward an η^1 bonding mode, which increases the elec-

(12) Finke, R. G.; Keenan, S. R.; Schiraldi, D. A.; Watson, P. L. *Organometallics* **1986**, *5*, 598.

(13) McDowell, S. A. C.; Amos, R. A.; Handy, N. C. *Chem. Phys. Lett.* **1995**, *235*, 1.

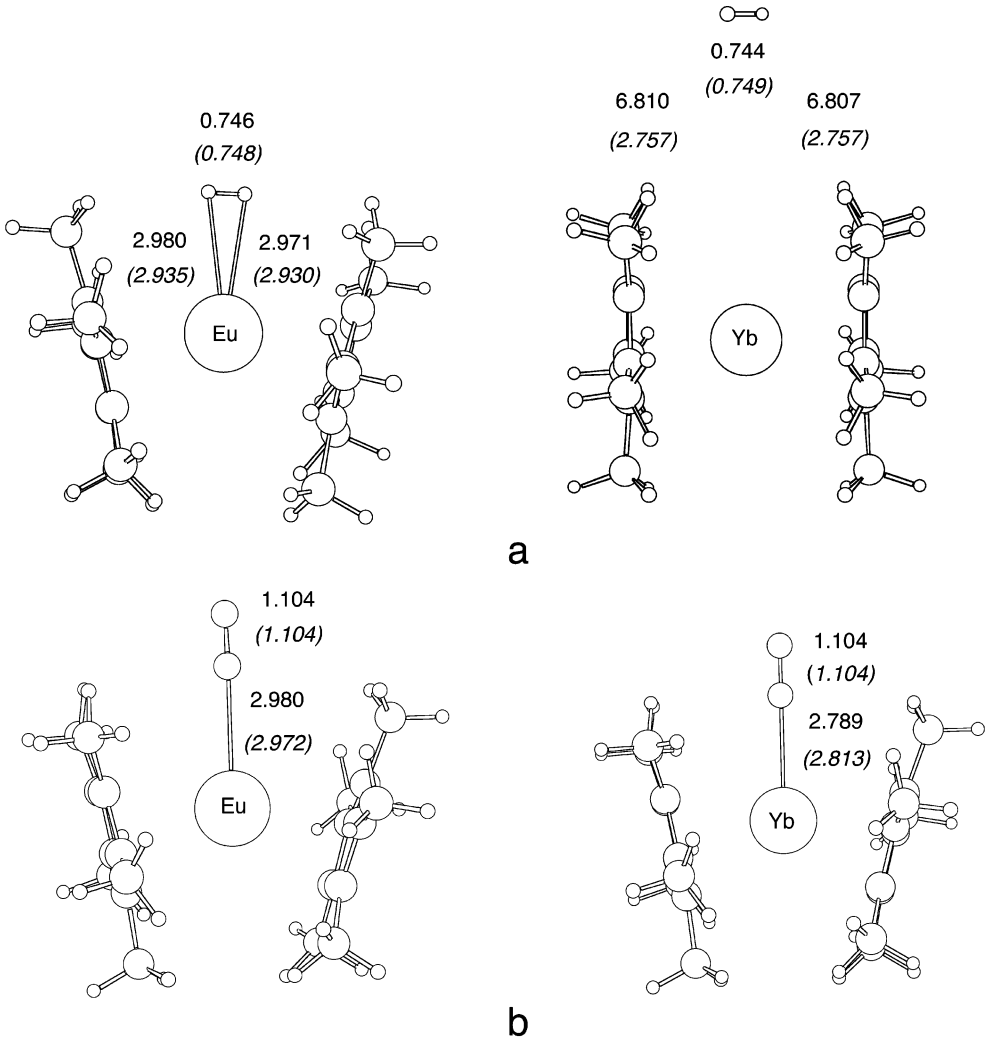

Figure 1. Optimized geometries of adducts of Cp^*_2Ln and Cp_2Ln (Ln = Eu, Yb) with (a) H_2[8] and (b) N_2. Distances are given in Å. Values in parentheses and italics are for Cp. Calculated distances for free ligands: H−H = 0.743 Å; N−N = 1.104 Å.

trostatic interaction with Cp_2M and Cp^*_2M through static polarization of H_2, illustrated as $M^{\delta+}\cdots H^{\delta-}H^{\delta+}$. The binding energies are related to the extent of bending and the resulting dipole moment in the Cp_2M fragment. The calculated dipole moment of Cp_2Eu (2.2 D for a Cp−Eu−Cp angle of 168° and 1.7 D for Cp^*_2Eu for an angle of 159°) is substantially larger than for Cp_2Yb (0.14 D) and Cp^*_2Yb (0.0 D) for angles of 179 and 180°, respectively.

(b) Dinitrogen. Dinitrogen binds weakly to these metallocenes, and the geometry is end-on (Figure 1). The metallocene interacts with the electrons in the HOMO of N_2, which results in the occurrence of an induced dipole moment (static polarization) illustrated as $M^{\delta+}\cdots N^{\delta-}N^{\delta+}$. No significant dynamic polarization can occur, since the low-lying π system overlaps poorly with the empty orbitals of the metal. Dihydrogen and dinitrogen both interact with Cp_2M or Cp^*_2M via static polarization, but dynamic polarization only exists with H_2. The lack of variation on the N≡N stretching frequency, in contrast with the significant lowering of the H−H stretching frequency (Sm, Eu), points toward the dominant influence of dynamic polarization in the dihydrogen ligand.

(c) Ethylene and Acetylene. The calculated geometry of the complexes shows that the HOMO of ethylene and acetylene approaches the open wedge of the metallocene fragment (Figure 2). This maximizes the dynamic polarization of the ligand, due to the relatively high energy of their π-orbitals. The nature of the HOMO in N_2, C_2H_4, and C_2H_2 clearly controls the different orientations and the nature of the interaction: static polarization for N_2 and dynamic polarization for C_2H_4 and C_2H_2. From these results, it seems that variation in the stretching frequencies is mostly determined by the dynamic polarization, which involves the π-systems. In the case of acetylene, the two π-systems are involved, which may be the reason for its greater binding energy relative to C_2H_4. This is consistent also with the shorter M−L distance for C_2H_2 relative to C_2H_4.

It should be noted that ethylene and acetylene are found to be perpendicular to the mirror plane of the Cp_2M fragment; however, they are in the plane of the Cp^*_2M fragment, as found in $Cp^*_2Yb(\eta^2\text{-MeC}\equiv\text{CMe})$.[11] The latter orientation is preferred sterically, as shown in the calculations on Cp^*_2M. The calculated Yb−C(alkyne) distance is longer (3.14 Å with C−C = 1.215 Å) than in $Cp^*_2Yb(\eta^2\text{-MeC}\equiv\text{CMe})$ (2.85 ± 0.01 Å).

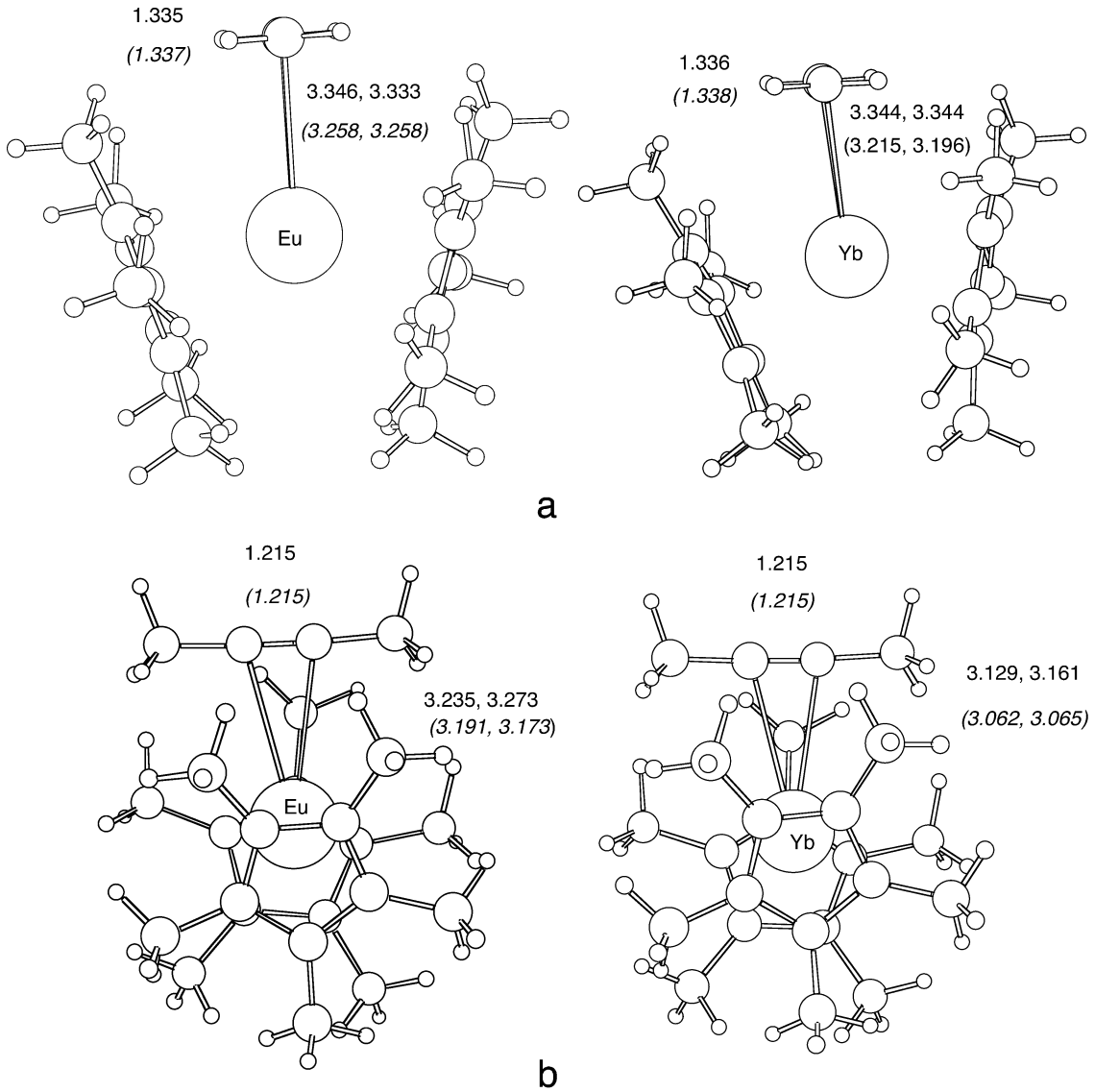

Figure 2. Optimized geometries of adducts of Cp^*_2Ln and Cp_2Ln (Ln = Eu, Yb) with (a) C_2H_4 and (b) C_2Me_2. Distances are given in Å. Values in parentheses and italics are for Cp. Calculated C−C distances for free ligands: C_2H_4, 1.330 Å; C_2Me_2, 1.210 Å.

(V) General Principles and Resulting Bonding Model. The general trend within the lanthanide metallocenes is that Cp_2Sm and Cp_2Eu tend to bind more strongly than the Yb analogue in all of the adducts considered. The calculations also document the effects of changing from Cp to Cp*, with the general result that the ligands bind slightly less well to Cp*M. This is perhaps due to the neutralization of the positive charge on M that increases by 0.1e, which weakens the donor−acceptor interaction. A question that naturally arises is why an interaction forms at all. DFT calculations underestimate dispersion forces,[3] and these are the dominant forces in these molecules. This is apparent in the comparison between the Yb−C(alkyne) distance in the calculated MeC≡CMe adduct of 3.12 Å and the experimental value of 2.85 ± 0.01 Å for the MeC≡CMe complex.

The following qualitative bond model may be advanced on the basis of the DFT calculations. The weak binding interaction results from a dipole-induced dipole interaction (static polarization) and from electron cloud deformation within the ligand by the electric field associated with the permanent dipole of the metal fragment (dynamic polarization). The bent-sandwich metallocenes have a permanent dipole moment in which the positive end is orientated along the *z* axis away from the bending. The ease of bending a metallocene fragment is related to the size of central metal atoms; those with larger radii are easier to bend, which in turn results in a larger permanent dipole moment. The calculated dipole moment is larger for Cp_2Eu or Cp^*_2-Eu and Cp_2Eu than for Cp^*_2Yb or Cp^*_2Yb, accounting for the slightly stronger interaction calculated for Eu relative to Yb.

As with CO bonding, these attractive interactions due to static and dynamic polarization must overcome the electron−electron repulsion of the electrons in the 4f shell, which is greater in Yb^{II} ($4f^{14}$) than in Sm^{II} ($4f^6$) and Eu^{II} ($4f^7$). Thus, the net bonding is a compromise between small attractive and repulsive forces, the net outcome of which is $\Delta E < 0$. Thus, the calculated energy changes that give rise to small bonding energies described here for molecular organometallic compounds

are, in a sense, like the "van der Waals forces" between atoms and/or nonpolar molecules in the gas phase.[14] If this is a good analogy, then the decamethylmetallocenes of the 4f block metals are good models for learning about the nature of weak metal−ligand bonds, in general.

Experimental Section

General Procedures. The experimental techniques used in this work were similar to those previously described.[15] All NMR solvents were dried and deoxygenated by distillation from sodium or potassium under nitrogen before use. The NMR experiments were done by dissolving $(Me_5C_5)_2Yb$ in the desired solvent, benzene-d_6, toluene-d_8, cyclohexane-d_{12}, or methylcyclohexane-d_{14}, in an NMR tube that was fitted with a J. Young valve which was used to connect the NMR tube to a small-volume vacuum line. The J. Young NMR tube was cooled in ice, or to a lower temperature, the contents of the NMR tube were exposed briefly to dynamic vacuum, and then the contents of the NMR tube were allowed to melt, while under static vacuum. This freeze−thaw procedure was repeated two more times. The NMR tube, while still in the cooling liquid, was isolated from the vacuum line, the small-volume vacuum manifold was filled to 1 atm with the desired gas, which expanded into the evacuated NMR tube, and the J. Young valve was closed. In this way, the pressure of gas in the NMR tube was slightly greater than 1 atm at room temperature. When the added ligand was a liquid, a similar transfer technique was used, except that the purified liquid was contained in a flask with a greaseless joint in order to connect the flask to the small-volume vacuum manifold. The vacuum manifold and the NMR tube were evacuated, and the contents of the flask containing the ligand were expanded into the manifold and attached NMR tube. Proton and carbon NMR spectra were recorded on a Bruker AMX spectrometer operating at 400 and 125.7 MHz, respectively, at the specified temperature.

Interaction of Cp^*_2Yb with H_2, Silanes, Methane, Olefins, and Xenon. Several experiments were done in which the perturbations of the ^1H and ^{13}C NMR chemical shifts of Cp^*_2Yb in the presence of various gases were monitored in cyclohexane-d_{12} at 25 °C. Placing an atmosphere of xenon over Cp^*_2Yb did not perturb the ^1H (1.871 ppm) and ^{13}C chemical shifts (114.32 and 10.60 ppm for the ring-C and the methyl-C resonances, respectively) relative to the values for the sample under dinitrogen; the chemical shift values were identical to within 1 and 10 ppb in the ^1H and ^{13}C NMR spectra, respectively. A similar lack of perturbation in the ^1H NMR spectra of Cp^*_2Yb was observed when the sample was exposed to dihydrogen, methane, and trifluoromethane; in each case the resonances due to the free ligands were observed at their unperturbed chemical shift values. In addition, the relaxation time, T_1, for free dihydrogen of 220 ms and the chemical shift of 4.54 ppm were identical with those of dihydrogen in the presence of Cp^*_2Yb. A sample of Cp^*_2Yb in benzene-d_6 was exposed to 1 equiv of 1,1,2,2-tetramesityldisilane in an NMR tube; no perturbation of the chemical shift of Cp*Yb or that of the free ligand and its J_{SiH} coupling constant was observed. A similar lack of perturbation on the chemical shift of Cp^*_2Yb in the presence of 1,1,1-tris(trimethylsilyl)dimethyldisilane was observed.

Exposure of Cp^*_2Yb in cyclohexane-d_{12} in an NMR tube at 25 °C to an atmosphere of ethylene produced polyethylene within minutes. On a synthetic scale, exposure of Cp^*_2Yb in pentane in a thick-walled pressure bottle to ethylene (12 atm) produced an immediate color change from orange to green and within seconds a precipitate of polyethylene formed. In a separate experiment, exposure of Cp^*_2Yb in pentane to CO (7 atm) resulted in a color change from orange to green. When this solution was exposed to ethylene (to a total pressure of 14 atm), no polyethylene was formed over a period of 1 h. A similar inhibition was observed when methane or xenon was used, but in these cases, no color change was observed and polyethylene was not formed within 1 h. In contrast, neither dihydrogen nor dinitrogen inhibits polyethylene formation under similar conditions. Exposure of Cp^*_2Yb in pentane to propylene (5 atm) did not result in a color change or polymer formation; when the pressure was released, the orange color reappeared and Cp^*_2Yb was recovered by crystallization. Exposure of Cp^*_2Yb to styrene (1 atm) resulted in a green solution, but no polystyrene formed.

Reaction of Cp^*_2Yb with Acetylenes. (a) With 2-Butyne. Decamethylytterbocene (0.22 g, 0.50 mol) dissolved in pentane (15 mL) was added to a degassed solution of 2-butyne (0.5 mL, 0.35 g, 6.5 mmol) in pentane (5 mL). The solution color changed immediately from orange to deep red. The volume of the solution was reduced to 5 mL, and the solution was cooled to −78 °C, resulting in formation of dark purple-red needles. When isolated and exposed to reduced pressure, the needles seemed to lose solvent, but they did not crumble or change color. The yield was 0.18 g (73%). Mp: 170−173 °C. Anal. Calcd for $C_{24}H_{36}Yb$: C, 57.9; H, 7.31. Found: C, 54.6; H, 7.33. ^1H NMR (C_6D_6, 30 °C): δ 1.99 (s, 30H), 1.27 (s, 6H). $^{13}C\{^1H\}$ NMR (C_6D_6, 30 °C): δ 113.4 (ring-*C*), 76.86 (*C*CH_3), 10.88 (ring-Me), 3.73 (C*C*H_3). ^1H NMR of 2-butyne (C_6D_6, 30 °C): δ 1.52. ^{13}C NMR: δ 74.60 (s) and 3.08 (q, $^1J_{CH}$ = 125 Hz).

(b) With Diphenylacetylene. This reaction was carried out in a manner similar to that described above. The adduct was isolated as black blocks from hexane at −25 °C in 91% yield. Mp: 121−123 °C. Anal. Calcd for $C_{34}H_{40}Yb$: C, 65.7; H, 6.50. Found: C, 64.9: H, 6.62. ^1H NMR (C_6D_6, 30 °C): δ 1.95 (s, 30H), 6.95 (m), 7.47 (m, the last two resonances give a combined integral of 10H). ^1H NMR of diphenylacetylene: δ 7.47 (m) and 6.98 (m).

(c) With 4,4-Dimethyl-2-pentyne. This reaction was performed in a manner similar to that described above. The adduct was isolated from a hexane solution at −25 °C as dark green-black feathers in 83% yield. Mp: 147−150 °C. Anal. $C_{27}H_{42}Yb$: C, 60.1: H, 7.86. Found: C, 59.1; H, 7.90. ^1H NMR (C_6D_6, 20 °C): δ 2.00 (s, 30H), 1,41 (s, 3H), 1.13 (s, 9H). ^1H NMR of 4,4-dimethyl-2-pentyne: δ 1.54 (s, 3H), 1.14 (s, 9H).

(d) With 1-Phenylpropyne. In a manner similar to that above, the adduct was isolated as dark brown-black needles in 85% yield. Mp: 126−129 °C. Anal. Calcd for $C_{29}H_{38}Yb$: C, 62.2; H, 6.86. Found: C, 61.8; H, 6.98. ^1H NMR (C_6D_6, 20 °C): δ 7.27 (m), 6.93 (m, the combined integral is 5H), 1.99 (30H), 1.48 (s, 3H). ^1H NMR of 1-phenylpropyne: δ 7.42 (m) 7.01 (m, the combined integral is 5H), 1.67 (s, 3H).

Computational Details. The Stuttgart−Bonn large core relativistic effective core potentials (RECPs) were chosen for the lanthanide centers.[16] For Eu and Yb, 10e large-core RECPs, adapted to the +II oxidation state of lanthanide, were used. Basis sets adapted to the RECPs were used. For Sm, Eu, and Yb, basis sets (7s6p5d1f) contracted in [5s4p3d1f] were used. C, N, and H were represented with a 6-31G(d,p) (double-ζ quality) basis set.[17] The C and H atoms of the Cp* methyl

(14) (a) Buckingham, A. D.; Fowler, P. W.; Hutson, J. M. *Chem. Rev.* **1988**, *88*, 963. (b) Bellert, D.; Breckenridge, W. H. *Chem. Rev.* **2002**, *102*, 1595.

(15) Schultz, M.; Burns, C. J.; Schwartz, D. J.; Andersen, R. A. *Organometallics* **2000**, *19*, 781.

(16) (a) Dolg, M.; Stoll, H.; Savin, A.; Preuss, H. *Theor. Chim. Acta* **1989**, *75*, 173. (b) Dolg, M.; Stoll, H.; Preuss, H. *Theor. Chim. Acta* **1993**, *85*, 441.

(17) Hariharan, P. C.; Pople, J. A. *Theor. Chim. Acta* **1973**, *28*, 213.

groups were represented with a 3-21G(d,p) basis set. Calculations were carried out at the DFT-B3PW91[18] level with Gaussian 98.[19] Geometry optimizations were carried out without any symmetry restrictions. The nature of the minima was verified with analytical frequency calculations.

Acknowledgment. This work was partially supported by the Director, Office of Energy Research, Office of Basic Energy Sciences, Chemical Sciences Division, of the U.S. Department of Energy, under Contract No. DE-AC03-76F00098. We thank the NSF for a fellowship (D.J.S.) and the Fanny and John Hertz Foundation for a fellowship (C.J.B.). We are grateful to the French computing centers CINES and CALMIP for a generous donation of computational time.

OM034206V

(18) (a) Becke, A. D. *J. Chem. Phys.* **1993**, *98*, 5648. (b) Burke, K.; Perdew, J. P.; Yang, W. In *Electronic Density Functional Theory: Recent Progress and New Directions*; Dobson, J. F., Vignale, G., Das, M. P., Eds.; Plenum: New York, 1998.

(19) Frisch, M. J.; Trucks, G. W.; Schlegel, H. B.; Scuseria, G. E.; Robb, M. A.; Cheeseman, J. R.; Zakrzewski, V. G.; Montgomery, J. A., Jr.; Stratmann, R. E.; Burant, J. C.; Dapprich, S.; Millam, J. M.; Daniels, A. D.; Kudin, K. N.; Strain, M. C.; Farkas, O.; Tomasi, J.; Barone, V.; Cossi, M.; Cammi, R.; Mennucci, B.; Pomelli, C.; Adamo, C.; Clifford, S.; Ochterski, J.; Petersson, G. A.; Ayala, P. Y.; Cui, Q.; Morokuma, K.; Malick, D. K.; Rabuck, A. D.; Raghavachari, K.; Foresman, J. B.; Cioslowski, J.; Ortiz, J. V.; Stefanov, B. B.; Liu, G.; Liashenko, A.; Piskorz, P.; Komaromi, I.; Gomperts, R.; Martin, R. L.; Fox, D. J.; Keith, T.; Al-Laham, M. A.; Peng, C. Y.; Nanayakkara, A.; Gonzalez, C.; Challacombe, M.; Gill, P. M. W.; Johnson, B. G.; Chen, W.; Wong, M. W.; Andres, J. L.; Head-Gordon, M.; Replogle, E. S.; Pople, J. A. *Gaussian 98*, revision A.9; Gaussian, Inc.: Pittsburgh, PA, 1998.